Measurements of the Laminar Burning Velocity of Ethanol-Water-Air Mixtures

R. Haas-Wittmüß, R.T.E. Hermanns*

OWI Oel-Waerme-Institut GmbH
Affiliated Institute of RWTH-Aachen, Germany

Abstract

The increasing interest in renewable fuels introduces new challenges in the different fields of combustion applications. With the introduction of biochemical derived fuels and impurities in it, validation is necessary to determine whether existing methods and models are usable for these bio-fuels. This research focuses on the combustion characteristics of ethanol-water-air mixtures. By using a modified Heat Flux burner the adiabatic laminar burning velocity is determined in a wide range of fuel-air-ratios and elevated temperatures and water contents. The stabilization of the approximately one-dimensional flame on a porous brass burner plate is performed under atmospheric conditions. The experimental results are in reasonable agreement to literature data and in good agreement with the detailed combustion reaction models of Leplat et al. and the San Diego mechanism.

Introduction

Renewable liquid fuels which are easily miscible with fossil liquid fuels and which additionally offer similar energy densities compared to fossil liquid fuels have significant advantages in compliances compared to other renewable liquid fuels. Hence, fuels with these prerequisites can play major role in a future energy supply. Due to the nature of these renewable fuels they can act as, so called, drop-in fuels. Hence, the introduction of these kind of renewable fuels can benefit from the well-established liquid fuel infrastructure. Alcohols derived through biochemical processes from biomass have the potential to provide such a renewable liquid fuel pathway, due to the oxygenated nature of alcohols these fuels they can act as renewable component for fulfilling legislative regulations. One such a fossil fuel substitute is ethanol, when produced from non-food-stock plants or waste. Due to the perfectly miscible character of ethanol and water it is generally difficult or costly to extract all the water by distillation. Furthermore, ethanol will absorb water as moisture from the air fast due to its hydrophilic nature. Both effects combined give a so called hydrated ethanol when used in appliances, which consists of about 5% water by volume.

By implementing ethanol as a fuel in combustion appliances it is clear that the properties related to the safety of burner devices will also change, e.g. ignition delay time, flame blow off and flame flash back. As a result, combustion properties have to be known for a wide operational range, since in practical appliances the fuel-air ratio, the pressure at which the combustion takes place, and the initial temperature of the combustible mixture may vary significantly from device to device. Among these combustion properties, the laminar burning velocity is one of the key parameters, which is a fundamental characteristic of the combustible mixture. Although a significant amount of experimental data of the laminar burning velocity of all kind of fuels is available in literature, the results exhibit some significant inconsistency. Even the spread of the measured values often exceeds the reported experimental uncertainty [13, 14]. Hence, new and accurate data for different fuels is invaluable for the design of combustion devices and validation of various models and reaction mechanisms. This was picked up recently by Beeckmann et al. [3] who tried to define some reference compositions and boundary conditions in order to identify the uncertainties of the different measurement methods with the goal to increase the accuracy of the determined experimental laminar burning velocity data.

The primary goal of the present study was to acquire new and accurate data of the laminar burning velocity of ethanol-water-air mixtures at elevated inlet temperatures. Additionally the experiments were performed to validate the adapted Heat Flux setup for liquid fuels and elevated inlet temperatures.

In the next section the developed and dedicated liquid fuel Heat Flux setup for elevated inlet temperatures is described. Followed by a brief explanation of the determination of both the laminar burning velocity. Since the experimental results are compared with numerical results, the applied combustion reaction mechanisms and numerical methods are also presented. The presented measurements are compared with experimental data from literature when available. This work is concluded with a discussion of the found results.

Experimental Details

The presented experiments are performed with the Heat Flux method, which is a well established method to determine the adiabatic laminar burning velocity. The method is discussed thoroughly in previous publications [4, 7, 14, 20] and should be consulted for a detailed description of the basic principles of the Heat Flux method. The experimental setup allows the measurement

*Corresponding author: r.hermanns@owi-aachen.de
Proceedings of the European Combustion Meeting 2015

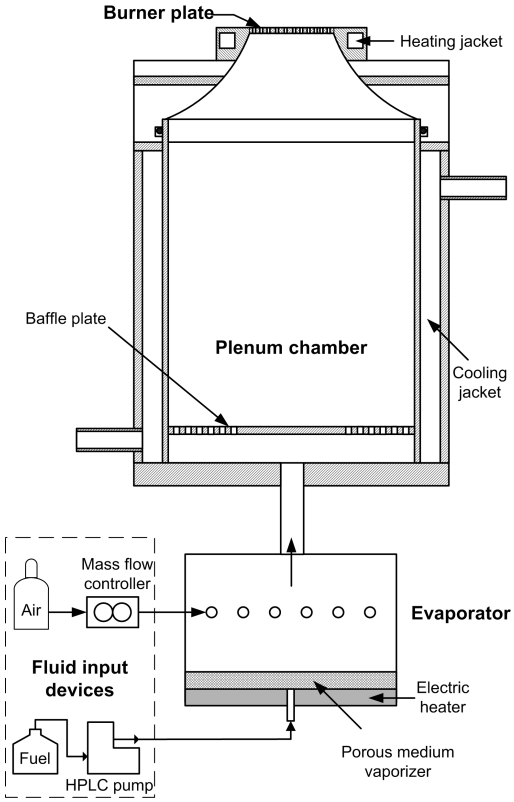

Figure 1: Schematic setup of Heat Flux burner showing its main components.

of the adiabatic laminar burning velocity by stabilizing a flat flame on a heated porous burner plate. The resulting flame can be assumed to be one-dimensional [21]. Additionally, de Goey [7] showed that the flame can be approximated as adiabatic due to the negligible heat loss of the flame.

The present experimental setup is very close to the original Heat Flux burner design of van Maaren [20], which was improved by Bosschaart [4]. Figure 1 shows a schematic representation of the Heat Flux burner setup used in the present research. Compared to the original design it is extended with an evaporator to convert liquid fuel to the gaseous phase. In this figure, four main components can be identified, the fluid input devices, the evaporator, the plenum chamber, and the burner plate. Detailed explanation of these new components follows below in order of the flow through the system.

The fuel-air-mixture is controlled by a mass flow controller and a high-performance liquid chromatography (HPLC) pump. In order to utilize liquid fuels, an accurate dosage system is necessary to provide a confident and steady fuel mass flow. In the present setup a HPLC pump, Type 305 by Gilson Inc., delivers a constant volumetric flow. The pump allows a fuel dosage of up to 25 mL/min with a minimal flow increment of 0.0025 mL/min. An additional pressure valve effectively damped the pumping fluctuations to a negligible level. The mass flow of the fuel is estimated by taking into account the temperature dependent density according to Golubev et al. [11]. The air flow is controlled by a mass flow controller. The error estimate of the air flow and fuel pump flow was identified to be 2.1 % and 1 % respectively of the set flow. The error estimate in density of the fuel itself is negligible. This adds to typical fuel equivalence ratio errors of approximately 3 %.

The liquid fuel is evaporated prior to mixing with the oxidizer. The vaporizer is a porous metal mesh disk, electrically heated. The fuel enters on the bottom of the disk and distributes inside due to capillary motion. The porous metal mesh of the evaporator acts as a buffer volume to further steady the fuel flow. The complete evaporation of the ethanol is ensured by temperature control of the metal vaporizer. The metal disk was kept at 90 ± 5 °C by manual control of the electric heater. The temperature of the air is preheated by passing a thermal oil thermostat, which also conditions the plenum chamber of the burner. The air enters the evaporator through a series of holes and generates a homogeneous mixture of fuel and air.

The premixed mixture is led towards the plenum chamber surrounded by a cooling jacket to provide temperature conditioning to the fuel-air-mixture. Before leaving the plenum chamber through the burner plate, with an effective diameter of 29.28 mm, the unburnt mixture temperature is recorded by a thermocouple. By varying the temperature of the thermal oil circuit and the electric energy supplied to the vaporizer, the mixture temperature is being controlled. Typical temperature variations of the premixed unburnt mixture are within 1 K, measured upstream but close to the burner plate.

Measurement Procedure

Standard procedure to measure the adiabatic laminar burning velocity of a fuel-air-mixture is to record the temperature profile on the burner plate for various gas velocities slightly above and below the estimated laminar burning velocity. An analytic analysis of the heat balance of the burner plate by van Maaren [20] showed that the recorded temperature profiles have a parabolic shape:

$$T_{\mathrm{p}}(r) = T_{\mathrm{c}} + \mathcal{C} r^2. \tag{1}$$

In this equation T_{p} is the plate temperature, T_{c} is a reference temperature measured at centre thermocouple, $\mathcal{C}$ the parabolic coefficient and r the radius at which the temperature is measured.

Modelling details

The experimentally determined laminar burning velocities are compared with numerical results. The freely propagating steady adiabatic premixed flames were modeled by using the multi-purpose flame code CHEM1D [6]. This code is based on a second-order exponential scheme to discretize the spatial derivatives in combination with

Table 1: Summary of laminar burning velocity experiments of ethanol-air flames available in literature. CF = Counterflow method; CV = Closed vessel method; HF = Heat flux method.

T_u (K)	p (atm)	ϕ	Method	Year	Refs
300-500	1-8	0.7-1.4	CV	1982	[12]
363-453	1	0.6-1.8	CF	1992	[8]
450	3	0.55-1.3	CV	2004	[10]
358-480	1	0.7-1.4	CV	2007	[16]
300-393	1-14	0.7-1.5	CV	2009	[5]
343	1	0.7-1.4	CF	2010	[22]
298-358	1	0.65-1.55	HF	2011	[14]
298,338	1	0.6-1.5	HF	2011	[19]
373	10	0.7-1.3	CV	2014	[2]
318-373	1	0.7-1.4	HF	Present work	

adaptive meshing and uses a modified damped Newton method to solve the resulting system of fully-implicit coupled nonlinear equations. Multi-component transport was modelled using the EGlib libraries [9]. Enthalpy fluctuations due to species diffusion (Sorret effect) and species diffusion due to temperature gradients (Dufour effect) are taken into account in this way. The total number of grid points was typically between 200-300.

The applied detailed reaction mechanisms are developed to predict flame properties of ethanol-air flames. Here these models are used to predict the burning velocity and effective activation energy. The first one is recently presented by Leplat et al. [15]. They checked the validity of their mechanism against experimental results (ethanol oxidation, ignition in a shock tube, combustion in premixed, partially-premixed, and non-premixed flames). This mechanism is designed for the modeling of combustion and oxidation of ethanol over the wide range of experimental conditions. The second applied combustion reaction mechanism is the San Diego mechanism version of 2012-09-07 [17]. The detailed chemistry applied in this mechanism is designed to focus on conditions relevant to flames, high temperature ignition and detonations. The number of species and reactions are kept to the minimum needed to describe the systems and phenomena addressed, thereby minimizing as much as possible the uncertainties in the rate parameters employed. An earlier version of this mechanism was validated against experimental data of ethanol flames [18].

Results

In Table 1 a summary of recently published experimental data of the laminar burning velocity of ethanol-air flames is listed. Various methods were utilized to determine the adiabatic laminar burning velocity of the fuel-air-mixtures at various conditions. Only a small set of the experimental data available in literature have exactly the same conditions which can be used for reference to compare and validate the present setup.

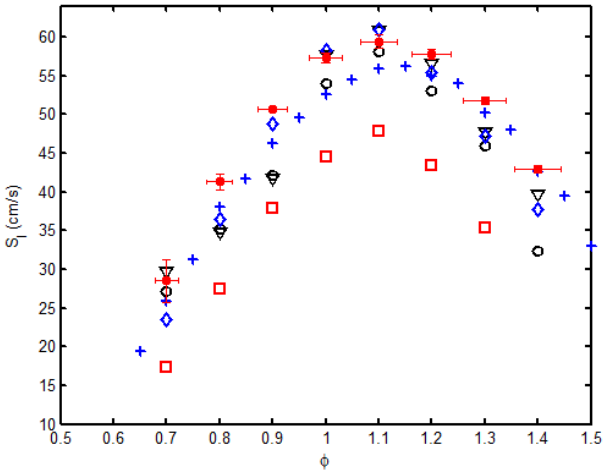

Figure 2: Laminar burning velocicties of ethanol-air flames as function of equivalence ratio at $p = 1$ atm and $T_u = 358$ K. The symbols denote: □, Bradley et al. [5]; +, Konnov et al. [14]; ○: Liao et al. [16]; ∇: Egolfopoulos et al. [8]; ◇, Gülder [12]; ■, Present work.

Therefore, in Fig. 2 the comparison is shown at a mixture temperature of $T_u = 358$ K and atmospheric pressure for various authors. The results of the experimental data of the adiabatic laminar burning velocity of the ethanol-air-mixture show an significant spread; more than 15 cm/s for various equivalence ratios, which is outside the experimental uncertainty of experimental setups. Especially the data of Bradley et al. [5] are significantly lower compared to the experimental data of other authors. The recently published data of Konnov et al. [14], Bradley et al. [5], Liao et al. [16], Egolfopoulos et al. [8] and the present results show no trend towards a statistically converged values of the laminar burning as a function of the fuel equivalence ratio. Generally the present results are on a high level compared to most of the other authors, although data of Bradley et al. [5] are comparable on the fuel rich side. Close to the stoichiometric value the present data are comparable to the experimental results of Egolfopoulos et al. [8] and Gülder [12]. This significant deviation in the laminar burning velocity affirms the need for new and accurate measured data.

A comparison of the applied combustion reaction models with new experimental data is shown in Fig. 3, where the adiabatic laminar burning velocities for different mixture temperatures ($T_u = 318, 358$ and 383 K) and water content in the fuel ($R_{H2O} = 0, 10$ and 20%) are plotted versus the equivalence ratio. Here, R_{H2O} is defined as the volume concentration of the fuel species water and ethanol (V_i) :

$$R_{H2O} = \frac{V_{H_2O}}{V_{C_2H_5OH} + V_{H_2O}} \cdot 100\%. \qquad (2)$$

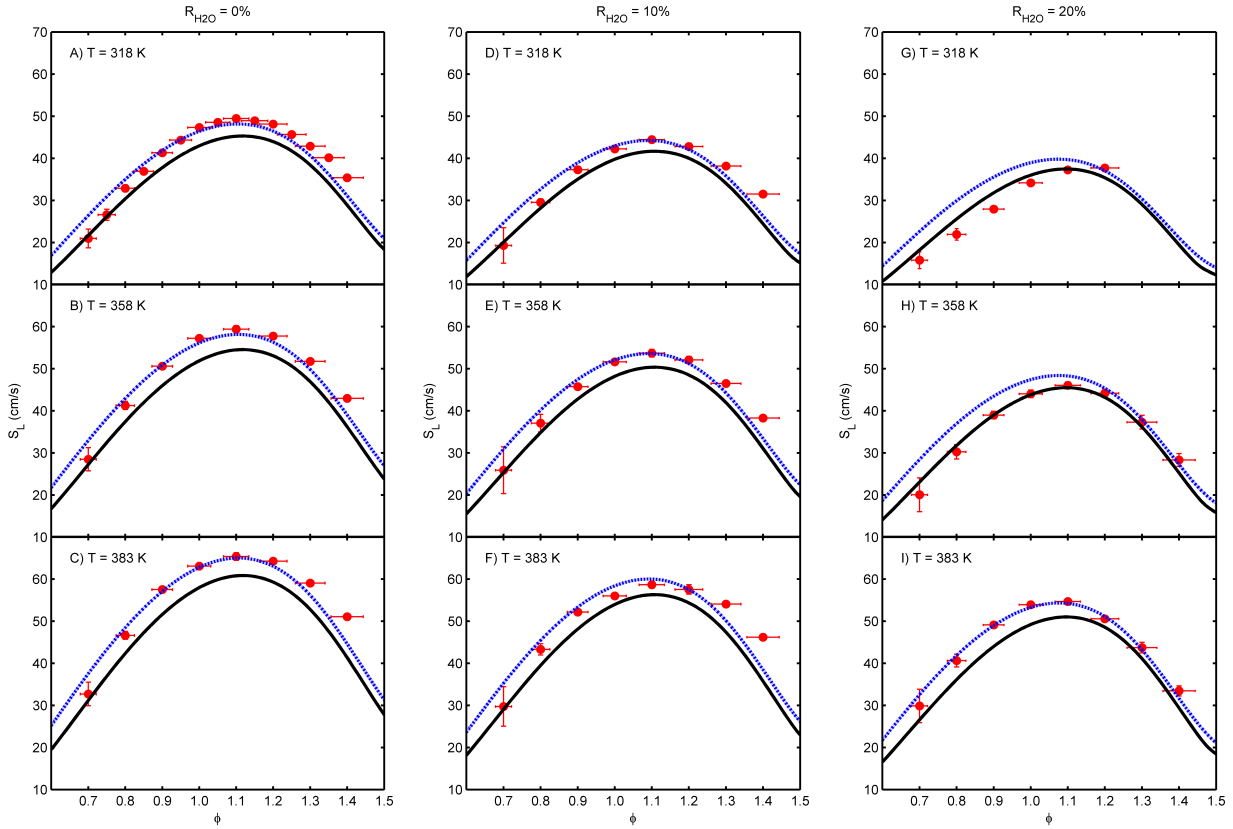

Figure 3: Measured laminar burning velocities with error estimates at atmospheric pressure and varying $T_{\mathrm{u}} = 318, 358$ and 383 K (rows) and varying $R_{\mathrm{H2O}} = 0, 10$ and 20% (columns) in comparison to numerical results as a function of the equivalence ratio. Symbols: Present work. Dashed-dotted line: San Diego mechanism[17], solid line: Leplat et al. mechanism [15].

The solid lines in the Fig. 3 represent the numerical results according to the reaction mechanism presented by Leplat et al. [15] and the dashes-dotted line show the results using the San Diego [17] combustion reaction mechanism. The present experimental results are presented with uncertainty estimates for S_L and ϕ. Overall the uncertainties in S_L are small, typically 0.8 cm/s, whereas the uncertainties in the fuel equivalence ratios are relatively large due to the large uncertainty in air supply (2.1%).

The San Diego mechanism [17] shows for $R_{\mathrm{H2O}} = 0$ and 10% and all temperatures (Figs. 3A-F) good agreement with the experimental results, whereas the mechanism of Leplat et al. [15] generally underpredicts the laminar burning velocity compared to the experiments. Overall, on the fuel lean side the reduction in S_L between $\phi = 0.8$ and $\phi = 0.7$ is underpredicted by both reactions mechanisms, whereas on the fuel rich side $\phi > 1.1$ the numerical results show a slightly faster decrease in S_L compared to the present experiments. The equivalence ratio of the maximum burning velocity for both experimental results and numerical data is slightly on the fuel rich side ($\phi \approx 1.1$) and generally do not differ much.

For $R_{\mathrm{H2O}} = 20\%$ and $T_u = 318$ and 358 K (Figs. 3G and H) the comparison between numerical data and experiments shows a different trend compared to the Figs. 3A-F. In Figs 3G and H the experimental data are even lower than the numerical data of Leplat et al. [15]. On the fuel rich side in Fig. 3H ($R_{\mathrm{H2O}} = 20\%$, $T_u = 358$ K) the comparison between experiments and numerical data are satisfactory. However, for $R_{\mathrm{H2O}} = 20\%$, $T_u = 383$ K (Fig. 3I) this different trend between experiment and numerical data is not visible any more and the results are in line with Figs. 3A and F.

Discussion

In order to get an understanding of this different trend between numerical and experimental data for $R_{\mathrm{H2O}} = 20\%$, $T_u = 318$ and 358 K (Fig. 3G and H) the fuel vaporization was analysed in detail. Fig. 4 shows the vapour-liquid phase behaviour of ethanol/water mixtures. Below the line with square symbols the mixture is completely in liquid phase, above the line with circle symbols the mixture is completely in vapour phase and in between the two lines a coexistent phase is present. If for example a mixture of $R_{\mathrm{H2O}} = 20\%$ (dashed vertical line denoted with symbol A) would be heated to the temperature of

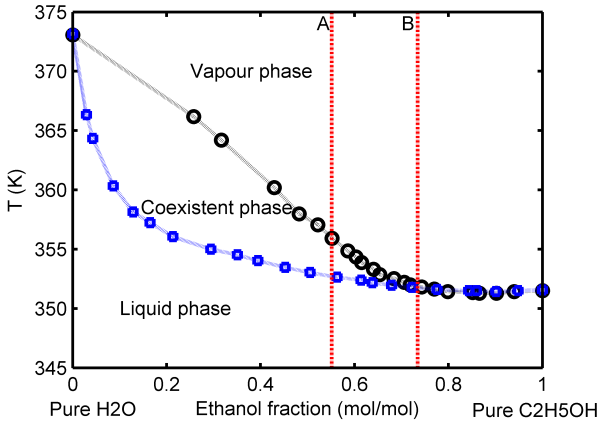

Figure 4: Vapour-liquid equilibrium mixture of ethanol and water at atmospheric pressure. Data taken from DDB [1]

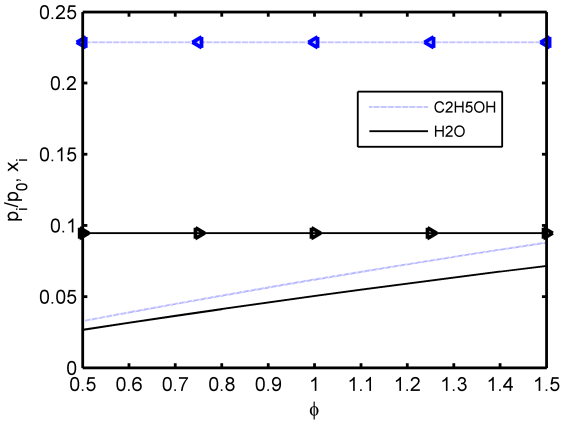

Figure 5: Fuel equivalence ratio as a function of the relative vapour pressure (p_i/p) and molar concentration x_i of ethanol and water at atmospheric pressure, $T_u = 318$ K and $R_{\mathrm{H2O}} = 20\%$. Lines with symbols: relative vapour pressure, lines without symbols molar concentration.

353 K, the mixture would consist of liquid with composition $R_{\mathrm{H2O}} = 20\%$ and vapour of composition at a temperature of 353 K but shifted towards lower R_{H2O} values. To avoid this coexistence and possible shift in composition between liquid and vapour phase the mixture has to be heated to a temperature where the mixture as a whole is in the vapour phase. For $R_{\mathrm{H2O}} = 10$ and 20% this means $T > 353$ and 357 K. For lower R_{H2O} values this coexisting phase for ethanol water mixtures is not possible any more.

By combining Raoult's and Dalton's law the relative vapour pressure (p_i/p) at which condensation can take place is being estimated under the assumption of ideal behaviour of Raoult's law for the ethanol-water mixture. The relative vapour pressure for atmospheric pressure and $T_u = 318$ K and $R_{\mathrm{H20}} = 20\%$ is shown in Fig. 5 (lines with symbols). Also, in this figure are the molar concentrations of water and ethanol which can be expected as a function of the fuel equivalence ratio (lines without symbols). From this figure it becomes clear that $p_i/p > x_i$ for water and ethanol for the complete range of measured equivalence ratios. This means that in principle no condensation can be expected. However, as is shown in Fig. 4 the temperature at which the fuel is vaporized should be at least 357 K for $R_{\mathrm{H2O}} = 20\%$ (denoted with A in Fig. 4). A local temperature drop of 8 K will decrease the relative vapour pressure (p_i/p) to values where condensation of water can take place for $\phi > 1.0$. Hence, the different trend between numerical and experimental data for $R_{\mathrm{H2O}} = 20\%$, $T_u = 318$ and 358 K can be explained by water condensation. In order to avoid this condensation in the future the setup has to be adjusted such that downstream of vaporizer a temperature exists which is high enough that no condensation can take place.

Conclusions

The present Heat Flux setup was successfully adapted for the measurement of the laminar burning velocities of liquid fuels at enhanced temperatures. The setup is carefully designed to minimize the uncertainties during the measurements. New and accurate data including error estimates are presented for the laminar burning velocity of ethanol-water-air mixtures at elevated temperatures and atmospheric pressure. The newly determined experimental data have been compared with both experimental data of other authors and recent combustion reaction mechanisms of Leplat et al. and San Diego [17]. It is shown that the scatter between recent experimental data available in literature is still significant. Hence, new data for ethanol-water mixtures is invaluable for the design of combustion devices and validation of various models and reaction mechanisms. In the two cases where some deviation is found between experimental data and numerical results it can be concluded that this results from condensation before entering the combustion chamber. Overall, the applied combustion reaction models show good results compared to the experimental data, especially the San Diego mechanism [17] agrees very well with present data.

References

[1] Dortmund Data Bank. Vapour-liquid equilibrium, 2014. Available at: http://ddbonline.ddbst.de/antoinecalculation/.

[2] J. Beeckmann, L. Cai, and H. Pitsch. Experimental investigation of the laminar burning velocity of

methanol, ethanol, n-propanol, and n-butanol at high pressure. *Fuel*, 117:340–350, 2014.

[3] J. Beeckmann, N. Chaumeix, P. Dagaut, G. Dayma, F. Egolfopoulos, F. Foucher, L.P.H. de Goey, F. Halter, A. Konnov, C. Mounaïm-Rousselle, H. Pitsch, B. Renou, E. Varea, and E. Volkov. Collaborative study for accurate measurements of laminar burning velocity. *Proceedings of the European Combustion Meeting*, (P3-76), June 25-28 2013. ISBN 978-91-637-2151-9.

[4] K.J. Bosschaart. *Analysis of the Heat Flux Method for Measuring Burning Velocities*. PhD thesis, Technische Universiteit Eindhoven, 2002.

[5] D. Bradley, M. Lawes, and M.S. Mansour. Explosion bomb measurements of ethanol-air laminar gaseous flame characteristics at pressures up to 1.4 mpa. *Combust. Flame*, 156:1462–1470, 2009.

[6] CHEM1D. *A one dimensional flame code*. Eindhoven University of Technology, 2002. http://www.combustion.tue.nl/chem1d.

[7] L.P.H. de Goey, A. van Maaren, and R.M. Quax. Stabilization of adiabatic premixed laminar flames on a flat flame burner. *Combust. Sci. Technol.*, 92:201–207, 1993.

[8] F.N. Egolfopoulos, D.X. Du, and C.K. Law. A study on ethanol oxidation kinetics in laminar premixed flames. *Proc. Combust. Inst.*, 24:833–841, 1992.

[9] A. Ern and V. Giovangigli. Eglib user manual, 1996. Available at: http://blanche.polytechnique.fr/www.eglib.

[10] J.T. Farrell, R.J. Johnston, and I.P. Androulakis. Molecular structure effects on laminar burning velocities at elevated temperature and pressure. *SAE Paper*, 1(2936), 2004.

[11] I.F. Golubev, T.N. Vasil'kovskaya, and V.S. Zolin. Experimental study of the density of aliphatic alcohols at various temperatures and pressures. *Inzhenerno-Fizicheskii Zh.*, 38:668–670, 1980.

[12] O.L. Gülder. Laminar burning velocities of methanol, ethanol and iso-octane-air mixtures. *Proc. Combust. Inst.*, 19:275–281, 1982.

[13] A.P. Kelley, Y.X. Liu, A.J. Smallbone, and C.K. Law. Laminar flame speeds, nonpremixed stagnation ignition, and reduced mechanisms in the oxidation of iso-octane. *Proc. Combust. Inst.*, 33:501–508, 2011.

[14] A.A. Konnov, R.J. Meuwissen, and L.P.H. de Goey. Temperature dependence of the laminar burning velocity of ethanol flames. *Proc. Combust. Inst.*, 33:1011–1019, 2011.

[15] N. Leplat, P. Dagaut, C. Togbe, and J. Vandooren. Numerical and experimental study of ethanol and oxidation in laminar premixed flames and in jet-stirred reactor. *Combustion and Flame*, 158:705–725, 2011.

[16] S. Y. Liao, D.M. Jiang, Z.H. Huang, K. Zeng, and Q. Cheng. Determination of the laminar burning velocities for mixtures of ethanol and air at elevated temperatures. *Applied Thermal Engineering*, 27:374–380, 2007.

[17] Mechanical and Aerospace Engineering (Combustion Research). Chemical-kinetic mechanisms for combustion applications. http://combustion.ucsd.edu, 2012.

[18] Priyank Saxena and Forman A. Williams. Numerical and experimental studies of ethanol flames. *Proceedings of the Combustion Institute*, 31(1):1149 – 1156, 2007.

[19] J.P.J van Lipzig, E.J.K. Nilsson, L.P.H. de Goey, and A.A. Konnov. Laminar burning velocities of n-heptane, iso-octane, ethanol and tertiary mixtures. *Fuel*, 90:2273–2781, 2011.

[20] A. van Maaren. *One-step chemical reaction parameters for premixed laminar flames*. PhD thesis, Technische Universiteit Eindhoven, 1994.

[21] A. van Maaren and L.P.H. de Goey. Laser doppler thermometry in flat flames. *Combust. Sci. Tech.*, 99(1–3):105–118, 1994.

[22] F.N. Veloo, P. Egolfopoulos. Studies of n-propanol, iso-propanol, and propane flames. *Combust. Flame*, 158:501–510, 2010.